Nanomechanics

DOI: 10.1002/anie.200900673

Understanding Covalent Mechanochemistry**

Jordi Ribas-Arino, Motoyuki Shiga, and Dominik Marx*

Most chemical reactions must be activated by some form of energy. The oldest approach is to use fire, that is, thermal energy leading to thermochemistry, but other "chemistries" are activated by light or electricity, that is, photochemistry or electrochemistry. In general, different ways of activation lead to different reaction pathways and products. A prominent example are pericyclic reactions, which are either thermochemically or photochemically forbidden or allowed, according to the Woodward–Hoffmann rules.[1] Although pioneering work dates back more than a century,[2] the field of mechanically induced covalent chemistry, dubbed here "covalent mechanochemistry", is still in its infancy.[3–5] Most recently, however, intriguing experiments have opened the door to applying forces on covalent bonds by exploiting atomic force microscopy (AFM),[6–9] force-clamp[10,11] and sonochemical[5,12,13] techniques. Despite promising case studies,[6,14–20] theory is in arrears when it comes to understanding the underlying concepts of nanomechanics. Here, we devise a most general theoretical framework that allows one to investigate covalent mechanochemistry both in terms of concepts and applications. This is achieved by exploiting the notions of force-transformed potential energy surfaces connected by Legendre transforms and isotensional versus isometric activation of covalent bonds, and by generalizing Fukui's Intrinsic Reaction Coordinate concept[21] to embody mechanical forces. Using a cyclobutene derivative[12,5] as a demonstration we delineate the limits of commonly used models, find topological rules that explain why certain pathways are mechanochemically allowed or forbidden, uncover differences between isotensional and isometric activation, and find topological irreversibility in stretching–compression cycles.

Atomic-scale manipulation using external mechanical forces has been used for about a decade now to stretch molecules in order to break their covalent bonds. Using AFM, force versus extension curves are measured by pulling apart chain molecules anchored both at the tip and to a support surface.[22] Theory mimicks this readily by imposing a distance constraint $q(\boldsymbol{x}) = |\boldsymbol{x}_i - \boldsymbol{x}_j|$ connecting two atoms at positions $\mathbf{x}_i$ and $\mathbf{x}_j$ and minimizing the function $V_{\mathrm{COGEF}}(\boldsymbol{x},q) = V_{\mathrm{BO}}(\boldsymbol{x}) - \lambda(q(\boldsymbol{x}) - q_0)$ (λ being a Lagrange multiplier) given a fixed value q_0 of the control parameter. Here, $V_{\mathrm{BO}}(\boldsymbol{x})$ is the ground-state Born–Oppenheimer potential energy surface (PES) as a function of all nuclear Cartesian coordinates $\boldsymbol{x}$ in the absence of any constraints. This constrained minimization yields not only the "COnstrained Geometries simulate External Force" (COGEF) potential[6,23] $V_{\mathrm{COGEF}}(q_0)$ as a function of q_0, but also the distorted molecular structures $\boldsymbol{x}_0(q_0)$ as well as force/extension curves $F(q_0)$. A closely related technique to account for finite temperature effects in the context of ab initio molecular dynamics has been presented in reference [17].

More recently, novel nanomechanical experimental approaches have been devised in which it is the force that is the control parameter, applied directly to selected atoms or functional groups. In force-clamp AFM experiments, for instance, properties such as catalytic activity are found to change in the presence of a constant external force.[10,11] Alternatively, forces can also be applied to molecules in isotropic solution by incorporating suitable mechanophores that convert mechanical energy into force,[5,12,13] much like chromophores convert light energy into electronic excitations. The common feature of such experiments is that inevitably the chemistry is altered when mechanical forces are applied.

Guided by the fundamental paradigm that the PES governs chemistry in a broad sense, the starting point must be a general approach to directly investigate how the PES changes as a function of applied mechanical forces $\boldsymbol{F}_0$ taking on the role of the control parameter, rather than indirectly by means of a structural constraint q_0. The basic notion that such forces affect the PES "by somehow tilting it" is old and can be traced back to early phenomenological work.[24] However, in the framework of electronic structure methods an exact, fully nonlinear, and self-consistent approach can be formulated by applying the external force directly on the respective atoms by minimizing the function outlined in Equation (1)

$$V_{\mathrm{EFEI}}(\boldsymbol{x},\boldsymbol{F}_0) = V_{\mathrm{BO}}(\boldsymbol{x}) - \boldsymbol{F}_0\,\boldsymbol{q}(\boldsymbol{x}) \tag{1}$$

with respect to $\boldsymbol{x}$ by structure optimization. Here, $\boldsymbol{F}_0$ is the constant external force associated with some structural parameter $\boldsymbol{q}$, as it is a generalized coordinate in terms of $\boldsymbol{x}$. At stationarity $\nabla_{\mathrm{x}} V_{\mathrm{EFEI}}(\boldsymbol{x}_0,\boldsymbol{F}_0)\,|_{\boldsymbol{F}_0} \overset{!}{=} 0$ for fixed $\boldsymbol{F}_0$ so that the external force $\boldsymbol{F}_0$ exactly cancels the internal force

---

[*] Dr. J. Ribas-Arino, Dr. M. Shiga,[+] Prof. Dr. D. Marx
Lehrstuhl für Theoretische Chemie
Ruhr-Universität Bochum
44780 Bochum (Germany)
E-mail: jribasjr@yahoo.es

[+] Permanent address: Center for Computational Science and
E-Systems, Japan Atomic Energy Agency (JAEA)
Higashi-Ueno 6-9-3, Taito-ku, Tokyo 110-0015 (Japan)

[**] We are grateful to Christof Hättig and Arnim Hellweg for technical help with TURBOMOLE and to Harald Forbert for useful discussions. We thank the Deutsche Forschungsgemeinsschaft (Reinhart Koselleck Grant to D.M.), the Alexander von Humboldt Stiftung (Humboldt Fellowships to J.R.A. and M.S.), the Catalan Government (Beatriu de Pinós Fellowship to J.R.A.), and the Fonds der Chemischen Industrie (D.M.) for partial financial support. The calculations were carried out using resources from BOVILAB@RUB and Rechnerverbund-NRW.

Supporting information for this article is available on the WWW under http://dx.doi.org/10.1002/anie.200900673.

$\boldsymbol{F} = -\nabla_q V_{\mathrm{BO}}(\boldsymbol{x}_0)$ at the determined minimum $\boldsymbol{x}_0$ and thus $\boldsymbol{q}(\boldsymbol{x}_0) = \boldsymbol{q}_0$ is obtained. This technique, where the "External Force is Explicitly Included" (EFEI), yields the exact distortion of the molecular structure, $\boldsymbol{x}_0(\boldsymbol{F}_0)$, in the full-dimensional $\boldsymbol{x}$-space as a function of the control parameter, $\boldsymbol{F}_0$. One can show that, at stationarity, $V_{\mathrm{EFEI}}(\boldsymbol{F}_0)$ is the Legendre transform of $V_{\mathrm{COGEF}}(\boldsymbol{q}_0)$ [Eq. (2)],

$$V_{\mathrm{EFEI}}(\boldsymbol{F}_0) = V_{\mathrm{COGEF}}(\boldsymbol{q}_0) - \boldsymbol{F}_0\, \boldsymbol{q}_0 \tag{2}$$

and that $\boldsymbol{F}_0$ and $\boldsymbol{q}_0$ can be considered to be conjugate variables (intensive and extensive, respectively) after $V_{\mathrm{COGEF}}(\boldsymbol{q}_0)$ is generalized to many dimensions. Most importantly, $V_{\mathrm{EFEI}}(\boldsymbol{x},\boldsymbol{F}_0)$ is the correct force-transformed Born–Oppenheimer PES and $\boldsymbol{x}_0(\boldsymbol{F}_0)$ describes exactly the deformation of the molecular structure $\boldsymbol{x}_0$ as a function of a specified external force $\boldsymbol{F}_0$. This allows one to evaluate, without invoking any approximation, properties such as reactant and transition state (TS) structures, $\boldsymbol{x}^{\mathrm{R}}(\boldsymbol{F}_0)$ and $\boldsymbol{x}^{\mathrm{TS}}(\boldsymbol{F}_0)$, or activation energies $E^{+}(\boldsymbol{F}_0)$ as functions of $\boldsymbol{F}_0$.

For our model system, *cis*-1,2-dimethylbenzocyclobutene, the activation energy E^{+} for electrocyclic ring-opening in the electronic ground state is found to be lower in the conrotatory than in the disrotatory pathway in the absence of force, as predicted by the Woodward–Hoffmann rules.[1] This traditional picture changes according to Figure 1 if a force F_0 exceeds a critical value of 0.51 ± 0.004 nN: the thermally forbidden disrotatory mechanism becomes mechanochemically allowed, in agreement with experiment.[12] Much more drastic is the finding that the conrotatory reaction channel even disappears altogether if the force exceeds 0.75 ± 0.004 nN. This heralds a radical change in the topology of the force-transformed PES. Finally, $V_{\mathrm{EFEI}}(F_0)$ also predicts that the disrotatory reaction even becomes barrierless at forces exceeding 3.09 ± 0.04 nN, whereas the molecule disintegrates beyond 6.51 ± 0.08 nN. Thus, applying forces in the 3.1–6.5 nN regime on C1 and C2 leads to a selective, purely mechanochemical cleavage of the C3–C4 bond, albeit along the thermally forbidden disrotatory pathway, without breaking the molecule apart. It is noted that the order of magnitude of such forces sufficient to manipulate covalent bonds is determined by their typical bond energy and length, that is, ≈1 eV per 1 Å or roughly 2 nN; this is in agreement with AFM measurements[3,6,9] that yield rupture forces of 2.6 to 13.4 nN for C–C bonds (see Table 3 in Ref. [3]).

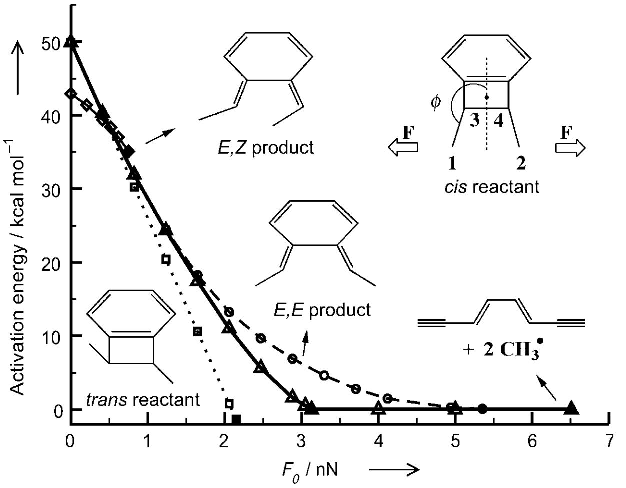

Figure 1. Force-dependence of the activation energies of the conrotatory (◇) and disrotatory (△) ring-opening processes of *cis*-1,2-dimethylbenzocyclobutene ("*cis* reactant") as calculated by the EFEI method. The force of magnitude F_0 is applied to atoms C1 and C2 along the interconnecting distance; insets show reactants, products, and the nomenclature. The points where the conrotatory channel disappears, the disrotatory pathway becomes barrierless, and where the molecule breaks apart (into C_8H_6 + $2\,CH_3^{\bullet}$) are highlighted by filled symbols. Along the disrotatory pathway the exact dependence (△) of the activation energy on the external force, that is, $E^{+}_{\mathrm{exact}}(F_0) = [V_{\mathrm{EFEI}}(\boldsymbol{x}^{\mathrm{TS}},F_0) - V_{\mathrm{EFEI}}(\boldsymbol{x}^{\mathrm{R}},F_0)]$, is compared to the predictions by Bell's model (□) and the tilted PES model (○; see the Supporting Information). Note: only the EFEI approach and thus $E^{+}_{\mathrm{exact}}(F_0)$ take self-consistently into account the distortion of all structures, in particular TS and R, due to external forces, as it is based on the proper force-transformed $V_{\mathrm{EFEI}}(\boldsymbol{x},F_0)$ potential, thereby generalizing the traditional formula $E^{+}_{\mathrm{exact}} = [V_{\mathrm{BO}}(\boldsymbol{x}^{\mathrm{TS}}) - V_{\mathrm{BO}}(\boldsymbol{x}^{\mathrm{R}})]$ without force to the case $F_0 > 0$ both exactly and straightforwardly.

However, $V_{\mathrm{EFEI}}(\boldsymbol{x},\boldsymbol{F}_0)$ is a high-dimensional hypersurface in coordinate space, which calls for simplifying analysis techniques. For such a task, one can generalize Fukui's Intrinsic Reaction Coordinate (IRC) concept[21] (which has proven valuable in the realm of thermochemistry) to covalent mechanochemistry by means of Equation (3),

$$\frac{d\tilde{\mathbf{x}}(s)}{ds} = -\frac{\nabla_{\tilde{\mathbf{x}}} V(\tilde{\mathbf{x}}(s))}{|\nabla_{\tilde{\mathbf{x}}} V(\tilde{\mathbf{x}}(s))|} \tag{3}$$

where $\tilde{\mathbf{x}}_i(s) = \sqrt{m_i}\mathbf{x}_i(s)$ are mass-weighted coordinates, s is the IRC "timestep", and V is $V_{\mathrm{EFEI}} = V_{\mathrm{BO}} - F_0 q$ or $V_{\mathrm{COGEF}} = V_{\mathrm{BO}} - \lambda(|\boldsymbol{q}| - q_0)$; here F_0 and q_0 are fixed whereas λ is determined at each step s to impose the constraint. This procedure yields properly force-transformed IRCs on EFEI or COGEF potential landscapes, respectively.

The surface $V_{\mathrm{EFEI}}(s,F_0)$ along the IRC for mechanochemical disrotatory ring-opening in Figure 2a quantifies how dramatically the external force F_0 distorts the potential energy landscape along the reaction coordinate s when compared to Fukui's thermochemical reaction profile, that is, $V_{\mathrm{BO}}(s) = V_{\mathrm{EFEI}}(s,F_0{=}0)$. Figure 2b demonstrates how the molecular structure is affected in terms of the conjugate variable to F_0: the C1–C2 distance, which is the mechanical coordinate q, is found to change by about 1.45 Å and 0.53 Å for reactant and product. Further unfolding of the EFEI hypersurface in terms of the C3–C4 distance and the rotation angle ϕ defined in Figure 1, reveals how the molecular structure responds to (i.e. strains resulting from) mechanical stress. Importantly, only IRCs obtained at sub-nN forces (such as in Figure 2d) are close to the path at zero force (see Figure 2c), whereas the reaction follows distinctly different pathways in the nano-Newton regime (see Figure 2e,f) as the molecular structure becomes extremely strained in this region. Underlying Bell's model,[25] however, is the assumption that the external force F_0 simply lowers the activation energy present in the absence of force by $E^{+}_{\mathrm{Bell}}(F_0) \approx E^{+}_{\mathrm{BO}}(F_0{=}0) - F_0\,\Delta q_{\mathrm{BO}}(F_0{=}0)$; here $\Delta q_{\mathrm{BO}}(F_0{=}0)$ is the change of the C1–C2 distance q in the TS relative to the reactant state at $F_0 = 0$. This widely used model is seen in

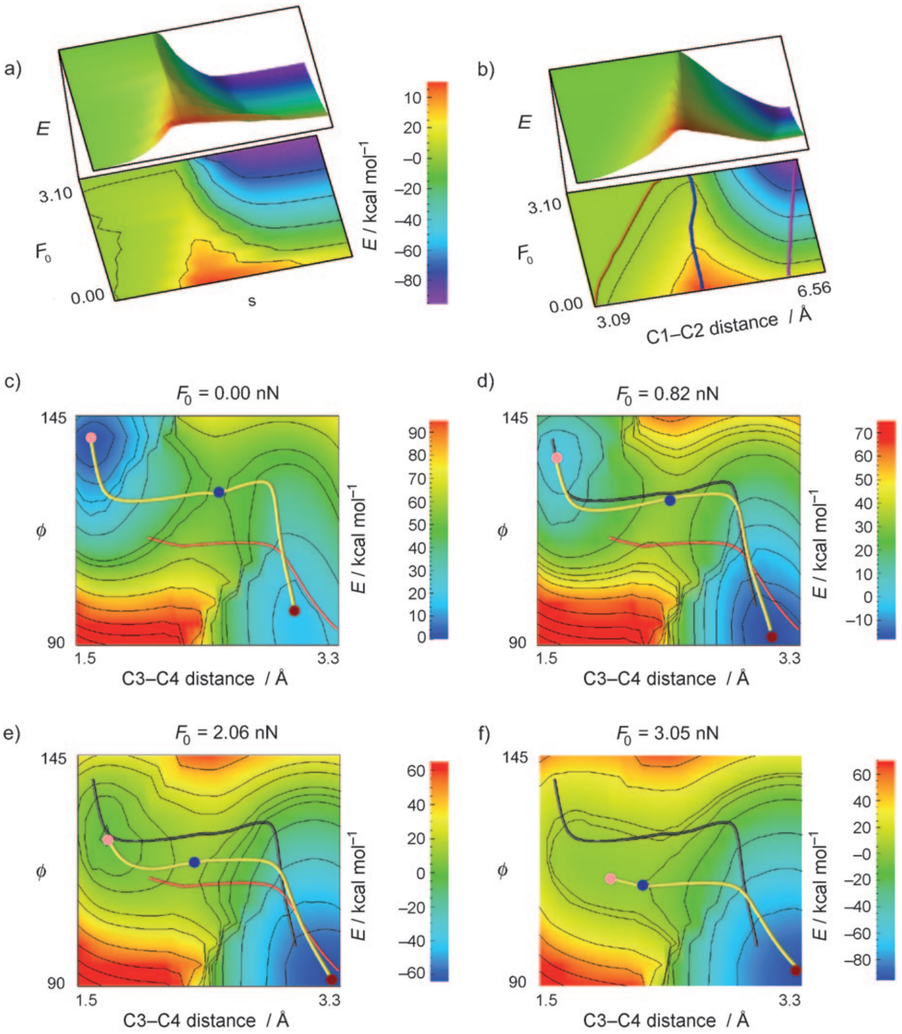

Figure 2. Force-transformed reaction profiles (a, b) and potential energy surfaces (c–f) for the disrotatory ring-opening of the *cis* reactant (see Figure 1); for details see the Supporting Information. Panel (a) shows how the standard thermochemical (Fukui) reaction profile at $F_0=0$, that is, the change of energy along the reaction coordinate *s*, is transformed when an external force $F_0>0$ is applied. Panel (b) shows how the energy changes because of the response of the variable conjugate to F_0, that is, the C1–C2 distance *q*, as a function of F_0. The red, blue, and magenta lines in (b) depict how the C1–C2 distance changes in the reactant, transition, and product states, respectively, as a function of F_0. Note the qualitative changes of these surfaces upon the application of external forces $F_0>0$ compared to $F_0=0$. Panels (c) and (d–f) show potential energy surfaces in the subspace spanned by two important internal coordinates, that is, the C3–C4 distance and the rotation angle ϕ (see Figure 1) at zero force and at finite forces, respectively. The force-transformed reactant-, transition-, and product-state configurations are marked by pink, blue, and brown points, respectively. The yellow curves correspond to the force-transformed IRC path at the given external force, whereas the black and red curves mark the IRC path at zero force (Fukui or thermochemical limit) and at maximum force (where the C3–C4 bond breaks), respectively.

Figure 1 to follow the exact EFEI result very closely up until $F_0\approx 0.5$ nN, before it fails dramatically beyond about 1 nN owing to its linear and non-self-consistent character. Still, this validates Bell's model when used in the sub-nN regime to extract Δq_{BO} values (i.e. the "Δx" or γ parameters) corresponding to the PES in the absence of force as achieved in recent constant-force AFM experiments.[10,11,26] In the more sophisticated tilted PES model,[27,28] $E^{\ddagger}_{\mathrm{t\text{-}PES}}(F_0)$ it is assumed that the force does affect structures, but it only shifts them along the IRC obtained at zero force. Such a posteriori "tilting" of BO profiles along the reaction coordinate works beyond Bell's regime up to about 1.5 nN, but breaks down beyond (see Figure 1). Therefore, although both models help to understand non-covalent mechanochemistry ruled by electrostatics, van der Waals forces, and hydrogen bonding, for example, in biophysics and polymer science, they both fail before reaching the realm of covalent mechanochemistry at several nano-Newtons.

Next, differences between isotensional and isometric covalent mechanochemistry are highlighted, stimulated by the distinct mechanical equations of state acquired when polymers are stretched.[29] Isometric stretching (red arrows) of the *cis* reactant in Figure 3a proceeds on its COGEF curve up to the point where it cannot sustain the pulling stress, and thus hops down at *constant* C1–C2 distance, that is, vertically, to the repulsive part of the *E*,*E*-product curve. Subsequent compression (turquoise arrows) starting from the *E*,*E*-product minimum is seen to drive the molecule back onto the repulsive part of the *E*,*E*-product curve, but from there it hops vertically down to the *trans* (!) reactant curve. The pathway of isotensional activation in Figure 3b is distinctly different involving for example, C1–C2 jumps as large as ≈2 Å. This manifests itself in qualitatively different isometric and isotensional force/extension curves (data not shown) as accessible by appropriate force spectroscopies.[6,7,10,11] Thus, in addition to different pathways, both isometric and isotensional stretching–compression cycles feature "topological irreversibility" as a result of the force-transformation of the Born–Oppenheimer PES.

What are now the rules that govern mechanochemistry? Figure 3a discloses that the COGEF curves of the *cis* reactant and *cis*-conrotatory TS never merge along *q*. Considering that in isometric conditions the transitions between COGEF curves must be vertical, we can conclude that the *E*,*Z*-product basin is topologically disconnected from the *cis* reactant, that is, the *E*,*Z* product is "mechanochemically forbidden" along this particular activation route *q*. In stark contrast, the *cis*-disrotatory TS does merge with the *cis*

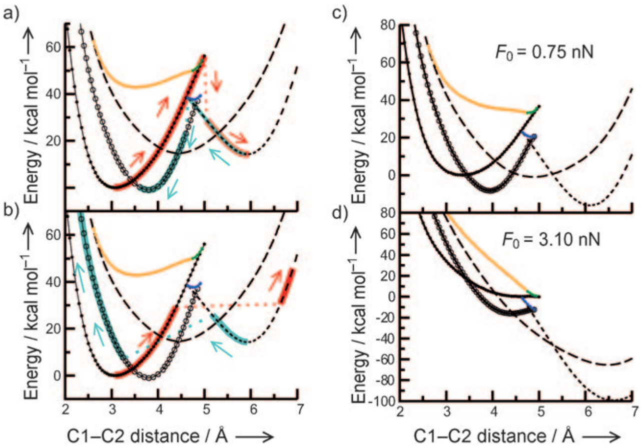

Figure 3. Trajectories followed by the system on the COGEF curves in isometric (a) and isotensional (b) stretching (red arrows) and compression (turquoise arrows) starting from the *cis* reactant (see Figure 1) as a function of the C1–C2 distance *q*; for details see the Supporting Information. Color code: *cis* reactant (black ●), *trans* reactant (black ○), *E*,*Z* product (long black dashed line), and *E*,*E* product (black dashed line) as well as *cis*-conrotatory (dotted orange line), *cis*-disrotatory (dotted green line), and *trans*-conrotatory (dotted blue line) TS. Panels (c) and (d) show force-transformed potentials at two different forces depicting the distortion of the potential energy landscape that leads to the disappearance of the conrotatory pathway from (b) to (c), and the cleavage of the C3–C4 bond yielding the *E*,*E* product (panel (d), see text).

reactant at $q \approx 4.90$ Å, thus leading to the mechanochemically allowed *E*,*E* product. Similarly, isometric compression of the *E*,*E* product connects its basin with the *trans*-conrotatory TS; however, it never merges with any *cis* TS. Thus, as ruled by topological bifurcations, the *trans*-reactant attractor is the mechanochemically allowed product upon compression whereas the *cis* attractor is forbidden. Isotensionally, the force-transformed curves in Figure 3c,d rationalize which reactions are allowed or forbidden by driving the molecule from minimum to minimum at constant external force. Figure 3c,d shows that the potentials of *cis* reactant and *cis*-conrotatory TS never merge for any F_0. Hence, the *E*,*Z* product is again mechanochemically forbidden, whereas the *cis*-disrotatory TS curve merges with the *cis* reactant at $F_0 \approx 3.10$ nN, thus the *E*,*E* product is again allowed. Finally, Figure 3c clarifies why the conrotatory pathway disappears for $F_0 > 0.75$ nN (see above): the *cis*-conrotatory state no longer features a minimum on the force-transformed potentials if $F_0 > 0.75$ nN. Instead, the force drives the system from the *cis*-conrotatory to the *cis*-disrotatory TS.

Clearly, the general framework provided here for molecular nanomechanics is a first step that must be extended to finite temperatures using free energy surfaces and Laplace transforms, torque and torsion, multireference electronic structure methods for bond breaking, and rigorous classification of force-induced bifurcations in terms of Thom's Catastrophe Theory using mechanical force as the proper control parameter.

Computational Section

All calculations were carried out using the B3LYP density functional together with Ahlrichs' SVP basis set. All techniques were implemented in TURBOMOLE or interfaced with it. Full methods and associated references are compiled in the Supporting Information.

Received: February 4, 2009

Keywords: computer chemistry · electrocyclic reactions · mechanochemistry

---

[1] R. B. Woodward, R. Hoffmann, *Angew. Chem.* **1969**, *81*, 797–869; *Angew. Chem. Int. Ed. Engl.* **1969**, *8*, 781–853.
[2] M. Carey Lea, *Philos. Mag.* **1892**, *34*, 46–50.
[3] M. K. Beyer, H. Clausen-Schaumann, *Chem. Rev.* **2005**, *105*, 2921–2948.
[4] S. Granick, S. C. Bae, *Nature* **2006**, *440*, 160–161.
[5] B. M. Rosen, V. Percec, *Nature* **2007**, *446*, 381–382.
[6] M. Grandbois, M. Beyer, M. Rief, H. Clausen-Schaumann, H. E. Gaub, *Science* **1999**, *283*, 1727–1730.
[7] T. Hugel, N. B. Holland, A. Cattani, L. Moroder, M. Seitz, H. E. Gaub, *Science* **2003**, *296*, 1103–1106.
[8] A.-S. Duwez, S. Cuenot, C. Jérôme, S. Gabriel, R. Jérôme, S. Rapino, F. Zerbetto, *Nat. Nanotechnol.* **2006**, *1*, 122–125.
[9] S. W. Schmidt, M. K. Beyer, H. Clausen-Schaumann, *J. Am. Chem. Soc.* **2008**, *130*, 3664–3668.
[10] A. P. Wiita, S. R. K. Ainavarapu, H. H. Huang, J. M. Fernandez, *Proc. Natl. Acad. Sci. USA* **2006**, *103*, 7222–7227.
[11] A. P. Wiita, R. Perez-Jimenez, K. A. Walther, F. Gräter, B. J. Berne, A. Holmgren, J. M. Sanchez-Ruiz, J. M. Fernandez, *Nature* **2007**, *450*, 124–127.
[12] C. R. Hickenboth, J. S. Moore, S. R. White, N. R. Sottos, J. Baudry, S. R. Wilson, *Nature* **2007**, *446*, 423–427.
[13] G. Cravotto, P. Cintas, *Angew. Chem.* **2007**, *119*, 5573–5575; *Angew. Chem. Int. Ed.* **2007**, *46*, 5476–5478.
[14] A. M. Saitta, P. D. Soper, E. Wasserman, M. L. Klein, *Nature* **1999**, *399*, 46–48.
[15] U. F. Röhrig, I. Frank, *J. Chem. Phys.* **2001**, *115*, 8670–8674.
[16] D. Aktah, I. Frank, *J. Am. Chem. Soc.* **2002**, *124*, 3402–3406.
[17] D. Krüger, H. Fuchs, R. Rousseau, D. Marx, and M. Parrinello, *Phys. Rev. Lett.* **2002**, *89*, 186402.
[18] M. K. Beyer, *Angew. Chem.* **2003**, *115*, 5062–5064; *Angew. Chem. Int. Ed.* **2003**, *42*, 4913–4915.
[19] D. Krüger, R. Rousseau, H. Fuchs, D. Marx, *Angew. Chem.* **2003**, *115*, 2353–2355; *Angew. Chem. Int. Ed.* **2003**, *42*, 2251–2253.
[20] M. Konôpka, R. Turanský, J. Reichert, H. Fuchs, D. Marx, I. Štich, *Phys. Rev. Lett.* **2008**, *100*, 115503.
[21] K. Fukui, *Acc. Chem. Res.* **1981**, *14*, 363–368.
[22] A. Janshoff, M. Neitzert, Y. Oberdörfer, H. Fuchs, *Angew. Chem.* **2000**, *112*, 3346–3374; *Angew. Chem. Int. Ed.* **2000**, *39*, 3212–3237.
[23] M. K. Beyer, *J. Chem. Phys.* **2000**, *112*, 7307–7312.
[24] W. Kauzmann, H. Eyring, *J. Am. Chem. Soc.* **1940**, *62*, 3113–3125.
[25] G. I. Bell, *Science* **1978**, *200*, 618–627.
[26] S. R. K. Ainavaparu, A. P. Wiita, L. Dougan, E. Uggerud, J. M. Fernandez, *J. Am. Chem. Soc.* **2008**, *130*, 6479–6487.
[27] E. Evans, K. Ritchie, *Biophys. J.* **1997**, *72*, 1541–1555.
[28] C. Bustamante, Y. R. Chemla, N. R. Forde, D. Izhaky, *Annu. Rev. Biochem.* **2004**, *73*, 705–748.
[29] D. Keller, D. Swigon, C. Bustamante, *Biophys. J.* **2003**, *84*, 733–738.